ISSN 2581 – 4303

Available Online at www.ijpba.info
International Journal of Pharmaceutical & Biological Archives 2019; 10(4):275-280

RESEARCH ARTICLE

Biofabrication of Silver Nanoparticles Using the Aqueous Extract of Weaver Ant's Nest and their *In Vitro* Cytotoxicity

Dineshkumar Sekar, Manikandan Dhanamoorthy, Chacko Vijai Sharma*

Department of Microbiology, K.M.G. College of Arts and Science, Vellore, Tamil Nadu, India

Received: 10 July 2019; Revised: 30 August 2019; Accepted: 16 October 2019

ABSTRACT

Environment has created creative and well-designed ways for developing nanomaterials having intriguing properties. Nanotechnology is having hope to open new avenues to combat and avert diseases using atomic-level fabrication of materials. Herein, we demonstrate the fabrication of silver nanoparticles using aqueous extract of weaver ant's (*Oecophylla smaragdina*) nest and its characterization using valuable techniques such as ultraviolet-visible spectroscopy, X-ray diffraction analysis, scanning electron microscopy analysis, Fourier-transform infrared spectroscopy, and atomic force microscopy analysis. Cytotoxicity of newly synthesized silver nanoparticles was analyzed using the Vero cells. By analyzing the results critically, it is hypothesized that synthesis and stabilization of silver nanoparticles were achieved using the molecules present in the aqueous extract of *O. smaragdina* nest.

Keywords: Atomic force microscopy analysis, nanomaterials, *Oecophylla smaragdina*, scanning electron microscopy analysis, silver nanoparticles, weaver ant

INTRODUCTION

Nanoscience has been recognized as an innovation for future society which will transform our lifestyle. Through the innovation of science and technology, the dimensions and property of nanoparticles have been understood. Nanoparticles have advantages over bulk materials due to their surface plasmon resonance (SPR), enhanced Rayleigh scattering, and surface-enhanced Raman scattering, quantum size effect in semiconductors supermagnetism in magnetic materials.[1,2]

Control over the dimensions of nanoparticles facilitates tuning of their optical, electronic, magnetic, and catalytic properties.[3,4] These pronounced effects of nanoparticles are arising from their extremely small sizes and large surface-to-volume ratio, large surface atom, large surface energy, spatial confinement, and reduced imperfections which are distinctively different from those of bulk ones.[5] Therefore, nanoparticles are regarded as building blocks of the next generation of drugs, optoelectronics, electronics, and various chemical and biochemical sensors.[1,2]

Biofabrication techniques have evolved in recent years as an effective, simple, and viable alternative to chemical and physical methods.[6-9] Green route synthesis of noble metal nanoparticles through biological process has attracted considerable interest. Such green route could provide the nanoparticles to more biocompatible and environmentally benign, cost-effective process and can be easily scaled up for a synthesis.[10,11] Herein, we report the synthesis and characterization of silver nanoparticles using an unusual source weaver ant's (*Oecophylla smaragdina*) nest. Before analyzing the biological properties, it is necessary to identify the cytotoxicity of synthesized silver nanoparticles. Hence, the *in vitro* cytotoxicity nature of synthesized silver nanoparticles was analyzed using Vero cells.

***Corresponding Author:**
Chacko Vijai Sharma,
E-mail: Chackosd1614@gmail.com

MATERIALS AND METHODS

Synthesizing material

The nest of the weaver ant *O. smaragdina* was collected from the neem tree in Vellore district.

Synthesis of silver nanoparticles using the nest of *O. smaragdina*

As a result of an extensive screening, the stock solution was fixed at the concentration of 100 mg of the nest of *O. smaragdina* in 10 ml of deionized water from the stock solution; different concentrations of nest extracts were mixed with different millimolar concentrations of silver nitrate solution. As a result, the synthesis of nanoparticles was achieved at the concentration of 0.7 mL of mangrove extract with 4.3 ml of 1×10^{-3} silver nitrate solution.

Characterization of silver nanoparticles

Ultraviolet (UV)–visible analysis

After reduction, the sample was collected and lambda max was measured in UV–visible spectroscopy. UV–visible graph was recorded using a quartz cuvette (4 cm × 1 cm × 1 cm). UV–visible analysis was carried out in Hitachi double beam UV–visible spectrophotometer (U-2800, Japan) and the reading was taken from 200 to 800 nm.

Scanning electron microscopy (SEM) analysis

SEM was used to know the surface deposited nanoparticles in our sample. After reduction, the sample was lyophilized and used for the SEM analysis. A carbon-coated membrane was placed on an aluminum disc and the sample smeared on the lining. An inert metal (gold) was coated using a sputter coater (cool sputter coat system model 5001, England) on the sample and this was placed inside the SEM (Leo Electron Microscopy Ltd., UK) at 20 kV. A tungsten electron gun releases a beam of electrons (primary electrons) that pass through a magnetic lense which scanning the surface of the sample. A beam of electrons (secondary electrons) was ejected from the surface of the sample, i.e., received by the electron amplifier. The amplified image was detected by photodetector and transferred to the computer screen.

Atomic force microscopy (AFM) analysis

AFM contains cantilever with a probe that is used to scan the surface of the specimen. The cantilever is made up of silicon or silicon nitride with a sharp probe. When probe is coming close proximity with the sample, makes the deflection on the cantilever based on the Hooke's law. Based on the situation, AFM measures contact force, van der Waals force, capillary forces, chemical bonding, electrostatic forces, magnetic forces, etc. It gives the three-dimensional images of the sample, which is the major advantage of AFM over other electron microscopes. After reduction, the thick smear of sample was done over the glass slide and it was air dried and then gone for the AFM analysis. AFM was done in Nanosurf Easyscan 2, Switzerland (Sanghi and Verma, 2008).

Fourier transform infrared (FTIR) analysis

The FTIR analysis was performed to study the presence of different functional groups in the sample. The lyophilized samples were subjected to FTIR studies in Thermo Nicolet Avatar 330 model diffuse reflectance mode at a resolution of 4 cm^{-1}. To obtain a good signal/noise ratio, 512 scans were recorded.

X-ray diffraction (XRD) analysis

This technique helps us to know the chemical composition and crystallographic structure of the sample. In this method, a monochromatic X-ray beam with wavelength lambda is projected onto a crystalline material at an angle theta. In our work, XRD is used to know the crystalline structure of the sample. The lyophilized samples were placed on the glass slide and gone for the XRD (Bruker, D8 advance, Germany) analysis to know the crystalline nature of our sample. The 2-theta values are taken from 10 to 90.

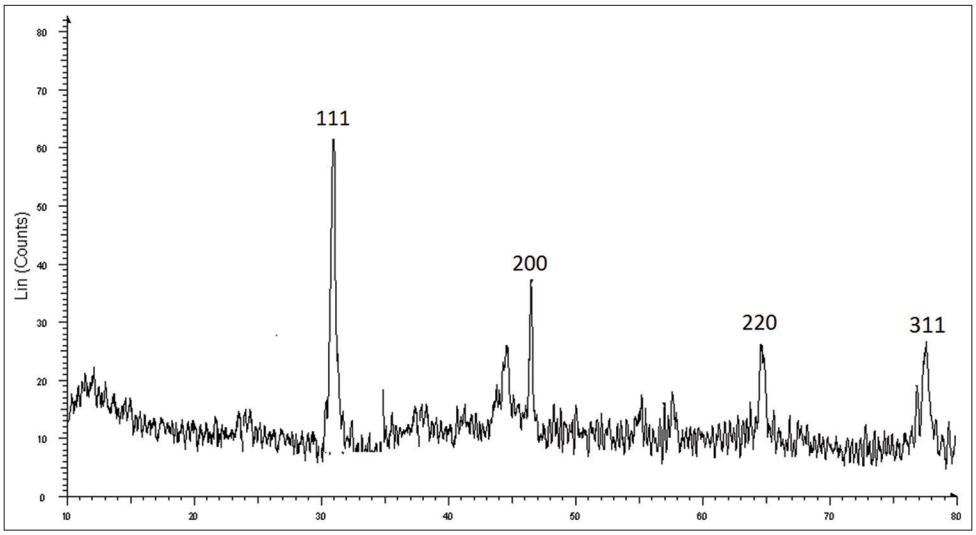

Figure 1: X-ray diffraction pattern of silver nanoparticles synthesized using *Oecophylla smaragdina* nest

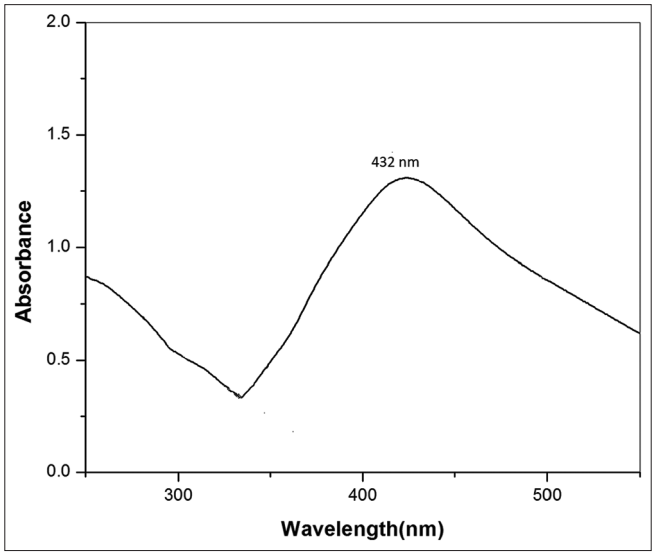

Figure 2: Ultraviolet–visible absorption spectrum of *Oecophylla smaragdina* nest synthesized silver nanoparticles

In vitro cytotoxicity assay

Cell lines and culture medium

Vero (Normal African green monkey) cells were cultured in SMEM supplemented with 10% inactivated fetal bovine serum (FBS)/newborn calf serum, penicillin (100 IU/ml), streptomycin (100 µg/ml), and amphotericin B (5 µg/ml) in a humidified atmosphere of 5% CO_2 at 37°C. The cells were dissociated with Trypsin Phosphate Versene Glucose solution (0.2% trypsin, 0.02% ethylenediaminetetraacetic acid, and 0.05% glucose in phosphate-buffered saline). The stock cultures were grown in 25 cm^2 culture flasks and all experiments were carried out in 96-well microtiter plates.

The monolayer cell culture was trypsinized and the cell count was adjusted to 1.0×10^5 cells/ml using SMEM medium containing 10% FBS. To each well of a 96-well microtiter plate, 100 µl of the diluted cell suspension was added. After 24 h, when a partial monolayer was formed, the supernatant was flicked off, the monolayer was washed once with medium and 100 µl of different nanoparticle concentrations (30, 45, 60, and 75 µg/ml) prepared in maintenance media were added per well to the partial monolayer in microtiter plates. The plates were then incubated at 37°C for 3 days in 5% CO_2 atmosphere. After 72 h, the 3-(4,5-dimethylthiazol 2-yl)-2,5-diphenyltetrazolium bromide (MTT) assay was carried out to identify the cytotoxicity nature of silver nanoparticles.

Statistical analysis

Every value was mentioned as mean ± standard deviation. SPSS software 15 for Windows (SPSS Inc., Chicago) was utilized for statistical analysis. Differences between the groups were established using one-way analysis of variance and $P < 0.05$ was considered statistically significant.

RESULTS AND DISCUSSION

Synthesis and characterization of silver nanoparticles using *O. smaragdina* nest extract

Biosynthesis of silver nanoparticles was accomplished using the nest of *O. smaragdina.* The distinct color changes colorless solution to yellowish brown in few

Figure 3: Fourier transform infrared spectrum of *Oecophylla smaragdina* nest synthesized silver nanoparticles synthesized silver nanoparticles

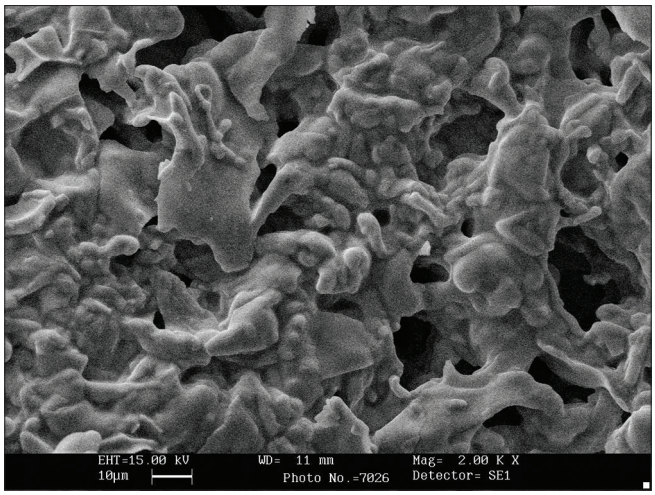

Figure 4: Scanning electron microscopy image of the newly synthesized silver nanoparticles using *Oecophylla smaragdina* nest

minutes of reaction then it indicates the formation of silver nanoparticles. Figure 1 shows characteristic SPR band at 432 nm and the yellowish-brown color in the reaction mixture is due to the surface plasmon vibrations of silver nanoparticles. The observed peak at 432 nm being a typical absorbance of silver nanoparticles confirms the formation [Figure 2].

FTIR spectroscopy studies on the silver nanoparticles synthesized using *O. smaragdina* nest extract

FTIR spectroscopy measurements were carried out to recognize the biomolecules that bound distinctively on the silver surface and involved in the synthesis of nanoparticles. Figure 3 represents that the band seen at 3446 cm^{-1} was assigned to the stretching vibration of primary amines. Another band seen at 1385 cm^{-1} corresponds to the C-N stretching of amines. This proves the presence of protein in the sample.

XRD measurements

The XRD pattern of the newly synthesized silver nanoparticles is shown in Figure 1. In XRD analysis, four peaks were identified at 2θ values of 30–80° set that the lattice planes were observed which may be indexed to the (111), (200), (220), and (311) reflections of face-centered cubic structures of silver (JCPDS File No: 04-0783 and 04-0784). In addition some unidentified peaks were also observed, which indicates the crystallization of bioorganic phase, occurring on the surface of silver nanoparticles which was crystalline in nature.

SEM

The scanning electron micrograph of the newly synthesized silver nanoparticles is shown in Figure 4. The image clearly shows that the nanoparticles are polydispersed.

AFM analysis

The silver nanoparticles were characterized by AFM for its detail size and morphology. AFM images were taken with silicon cantilevers with

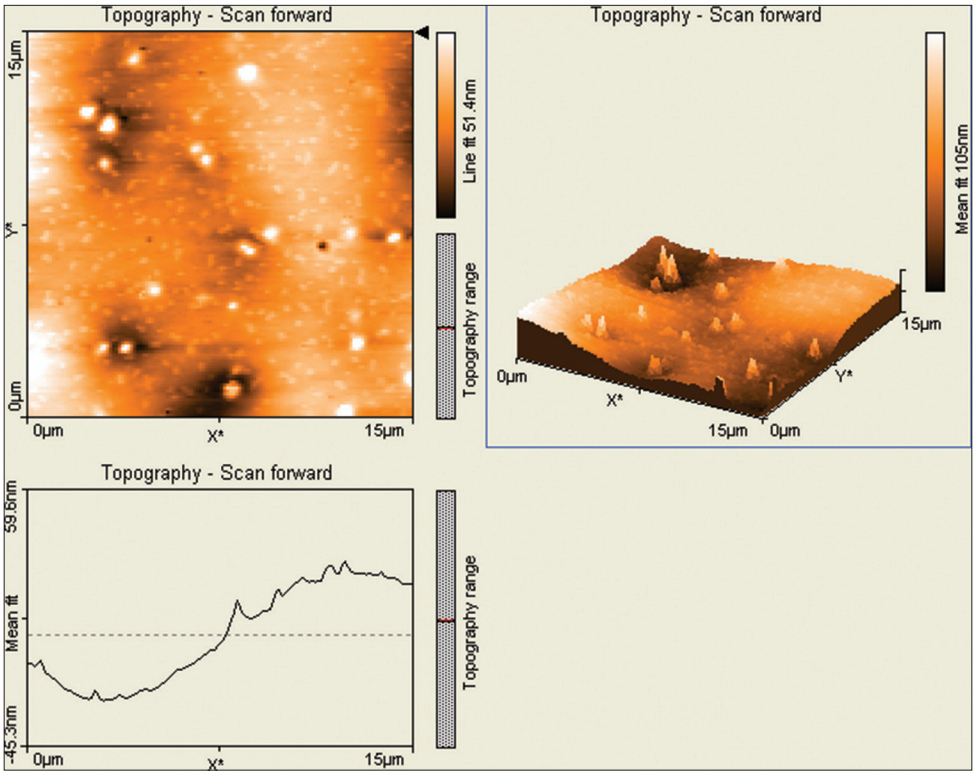

Figure 5: Atomic force microscopy image of the newly synthesized silver nanoparticles using *Oecophylla smaragdina* nest

force constant 0.02–0.77 N/m, tip height 10–15 nm, contact mode. It was noticed that the polydispersed silver nanoparticles were formed and it was in the range of 35–75 nm [Figure 5].

In vitro cytotoxicity assay

MTT assay was deployed here to analyze the cytotoxic nature of the *O. smaragdina* nest fabricated silver nanoparticles. The concentration required for trigger 50% cell death (CC_{50}) was 15.32 ± 0.4 µg/mL.

CONCLUSION

Silver nanoparticles were successfully synthesized using the nest of *O. smaragdina* and characterized using the standard techniques such as UV–visible spectroscopy, XRD analysis, SEM analysis, FTIR spectroscopy, and AFM analysis. The significance of these findings is arrived from its unusual biological source nest of *O. smaragdina*. Through the *in vitro* cytotoxicity assay, CC_{50} concentration was found to be 15.32 ± 0.4 µg/mL.

REFERENCES

1. Wong TS, Schwaneberg U. Protein engineering in bioelectrocatalysis. Curr Opin Biotechnol 2003;14:590-6.
2. Ramanaviciusa A, Kausaite A, Ramanaviciene A. Biofuel cell based on direct bioelectrocatalysis. Biosens Bioelect 2005;20:1962-7.
3. Liu H, Salabas EL, Schuth F. Magnetic nanoparticles: Synthesis, protection, functionalization, and application. Angew Chem Int Ed 2007;46:1222-44.
4. Ansari AA, Alhoshan M, Alsalhi MS, Aldwayyan AS. Prospects of nanotechnology in clinical immunodiagnostics. Sensors (Basel) 2010;10:6535-81.
5. Singaravelu G, Arockiamary JS, Kumar VG, Govindaraju K. A novel extracellular synthesis of monodisperse gold nanoparticles using marine alga, *Sargassum* wightii Greville. Colloids Surf B Biointerfaces 2007;57:97-101.
6. Mubarak-Ali D, Sasikala M, Gunasekaran M, Thajuddin N. Biosynthesis and characterization of silver nanoparticles using marine cyanobacterium *Oscillatoria willei* NTDM01. Dig J Nanomater Biostruct 2011;6:385-90.
7. Gangula A, Podila R, Ramakrishna M, Karanam L, Janardhana C, Rao AM, *et al.* Catalytic reduction of 4-nitrophenol using biogenic gold and silver nanoparticles derived from *Breynia rhamnoides*. Langmuir 2011;27:15268-74.
8. Sastry M, Ahmad A, Khan MI, Kumar R. Biosynthesis of metal nanoparticles using fungi and actinomycete. Curr Sci 2003;85:162-70.

9. Devi TB, Ahmaruzzaman M, Begum SA. A rapid, facile and green synthesis of Ag@AgCl nanoparticles for the effective reduction of 2, 4-dinitrophenyl hydrazine. New J Chem 2016;40:1497-506.
10. Prabhu S, Poulose EK. Silver nanoparticles: Mechanism of antimicrobial action, synthesis, medical applications, and toxicity effects. Int Nano Lett 2012;2:32-41.
11. Arunachalam KD, Annamalai SK, Hari S. One-step green synthesis and characterization of leaf extract-mediated biocompatible silver and gold nanoparticles from *Memecylon umbellatum*. Int J Nanomedicine 2013;8:1307-15.